Asian Power Electronics Journal, Vol. 13 , No.1, June 2019

Conceptual Design and Simulation for A Double-Rotor Switched Reluctance Motor Using Parallel Series Windings

Li S. Y [1] Cheng K. W. E [1] Zou Y [1]

Abstract–In this paper, an interchangeable parallel-series winding approach is used to realize a compact machine-housing proposed for the double-rotor motor, based on switched reluctance principle. First, theoretical analyses are elaborated for the concept of the design, combining with the magnetic circuit analysis and given a demonstration by using this approach. Second, the basic mathematical model for the motor is introduced and by using finite element method (FEM), the magnetic field distribution of the motor is acquired and collect torque data, followed by the coupling effects analysis that shows the decoupled magnetic circuits for the two rotors. Finally, to simulate the real working condition, the multi-physical domain simulation is carried out, and high and low speeding operations are obtained. It suggested that the motor is capable of realizing high and low speeds for continuously variable transmission and is expected to be employed by electric vehicles (EVs) and Electric Vessel in the future.

Keywords–Parallel-series-winding, double-rotor motor, switched reluctance, FEM, EVs.

I. INTRODUCTION

Electrical vehicles (EVs) have become a popular candidate for public transportation and many researchers have been investigating and developing, increasingly, under the background of green energy exploring and application. In order to realize a continuously variable transmission (CVT), some traditional EVs adopt intermediate parts such as mechanic and magnetic gears, hydraulic convertors and transferring belts, etc. for speed regulation. To eradicate these intermediate parts and enhance the efficiency for EVs, double-rotor motors have been investigated for EVs. Similar, Electric Vessel also requires the same requirement of transmission. The double-rotor motors have advantages of high traction torque-speed, compact volume and low cost, and most importantly, simultaneous high and low speeds operation [1]. Until now, there are mainly four types of double-rotor motors: direct current (DC) motor, double induction-rotor motor, double switching-flux rotors and double switched-reluctance-rotor motor [2-4]. The difference between the last two motors is that the last one does not own permanent magnets (PMs) [5]. However, all of them are simply designed by integrating two motors into a motor housing, therefore creating two rotors or stators on their corresponding windings. They are usually comprised by two electrical terminals that are roughly equivalent to two motors combining together. For example, ZiXuan's paper [6], has proposed a brushless permanent magnets double-rotors motor for a HEV, and there are two layers of windings with two electric ports for the stator. The same approach for a brushless direct current motor (BLDC) proposed by Durmus Uygun in [3] also simply integrates two DC motors together. In order to avoid the demagnetized influence of permanent magnets, switched reluctance double-rotor motors have been proposed in [7], [8] and this simple approach is employed again. On the other hand, the use of synchronous motor has been applied in vessel but the application to switched-reluctance motor for vessel is not yet reported. It is hard to realize a compact structure if we adopt the simple idea which integrates two identical or different type motors into one machine housing, for these motors are difficult for mass production due to their complex winding slots, and complex flux barriers that should also be taken into account.

Actually, it is essential and necessary by employing or designing simple structures not only for rotors but also for stators and windings as well to effectively realize a compact volume for double-rotor motors of EVs. In this paper, a double-rotor motor based on switched reluctance principle has been proposed. This motor, adopting only one layer of windings fixed on a stator, governs both outer rotor and inner rotor respectively. Put it in another way, both of the two rotors share the same windings to generate torques together. Therefore, the volume of the double-rotor motor can be significantly reduced and simultaneously, low speed and high-speed operations for this motor can be realized readily. Since this motor is a pure switched reluctance motor (SRM) without permanent magnets, it owns all merits that traditional SRMs possess. The paper includes the following contents. First and foremost, the concept of the design has been proposed and then, theoretical analyses are given by using magnetic circuit method so that they verify the effectiveness of the concept. Next, electromagnetic field of the motor are analyzed and calculated by finite element method (FEM), and magnetic coupling analysis is also carried out. Last but not least, a multi-physical field simulation is completed to emulate the real working condition for the motor, which shows the good performance of the motor. It testifies the effectiveness and feasibility of the proposed concept of the motor.

II. THEORETICAL ANALYSIS

1. Magnetic structure of the motor

This motor has two rotors including rotor 1 and rotor 2 shown in Fig.1. Rotor 1 owns a series of teeth that are distributed evenly around within the rotor. Rotor1, stator and rotor2 are comprised by stacked silicon steels. The stator has two poles with small teeth that are identical to that of rotor 1. A pair of coils is wrapped on the two poles for each stator and totally, there are six stators for the motor. Two opposite stators comprise a phase for the motor, which are similar to pure SRM. And all phases are allocated around the rotor 1 with nearly 60 mechanically interval degrees between two adjacent ones. More

[1] **Power Electronics Research Center, Department of Electrical Engineering, The Hong Kong Polytechnic University, HongKong**
E-mail: eric-cheng.cheng@polyu.edu.hk

importantly, as shown in this figure, phase B is aligned with both rotor1 and rotor 2 at the moment. Rotor 2 has two poles and, in the middle part of each pole, there is also a pole with a minimum thickness so that this rotor can realize two step alignments with different lengths of gaps. All rotors and stators are fixed on a shaft by using bearings that are not given in this figure.

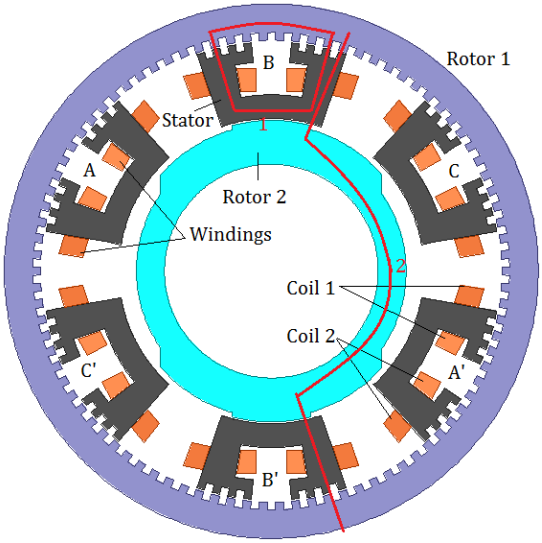

Fig. 1: The structure of the magnetic paths.

2. Theoretical concept

According to the minimum magnetic reluctance principle, the two rotors can be driven by the same stator with current carried windings. Both short flux and long flux paths exist in this motor and when rotor 1 is excited. Under the condition, flux lines would pass through stator to rotor 1 only, crossing the air gaps between them, as shown by the red closed line 1 in Fig.1. When phase AA', CC' and BB' are excited in sequence, the rotor 1 will rotate along anti-clockwise direction. The rotor 2 is driven by the same stators under the long-path flux lines that are shown in Fig.1 highlighted by red line 2. Coincidently, rotor 2 can also rotate in anti-clockwise when phase AA' CC' and BB' are excited in order. The key difference to drive the two rotors is the electric connecting way of the two coils (coil 1 and coil2).

The magnetic paths shown in Fig.1 can be simplified by Fig.2, taking phase BB' as an example. If the two coils of phase B are connected in a serial way and the magnetic circuit for the flux generated by the two coils are shown in the corner of Fig.2. There will be short flux lines passing along the rotor 1 and the stator only. These flux lines cannot influence the status of the rotor 2 because there are no flux lines along the rotor 2. The flux can be expressed as

$$\varphi_1 = \frac{F_1+F_2}{R_1+2(R_s+R_{g1})+R_y} \quad (1)$$

When the two coils of phase B are connected in parallel and then connected with that of phase B' in series, the magnetic circuit for the flux can be shown in Fig.2 and this long flux can be calculated by

$$\varphi_2 = \frac{F_1+F_3}{R_1'+R_s+R_{g1}+2R_{g2})+\frac{R_2}{2}} \quad (2)$$

Since the air gaps between the stator and rotor 1 are much smaller than that between the stator and the rotor 2, the flux lines are mainly influenced by the variations of the air gaps *Rg2*. More markedly, there are two different gaps between the stator and the rotor 2, for it has a pair of Y-shaped poles. Therefore, either phase A or phase C excited will drive the rotor to coincide with the central line of the poles, thus driving the rotor 2 rotating in anti-clockwise or clockwise respectively. Torque profiles for rotor 1 and rotor 2 will be discussed in the following part.

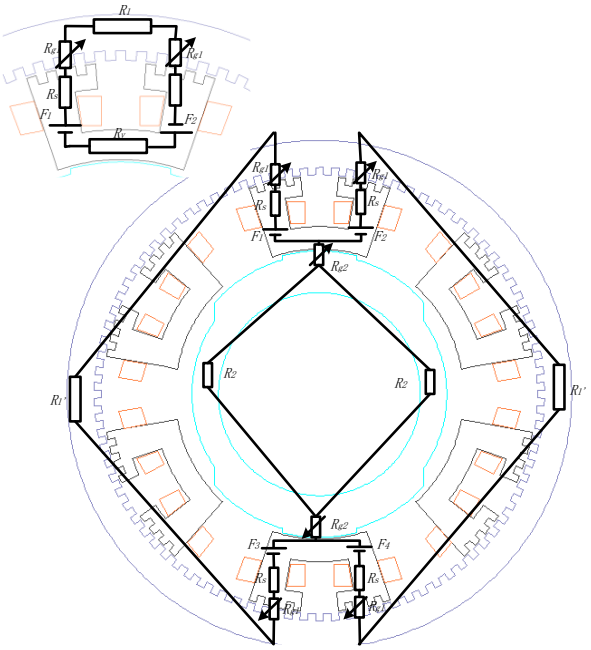

Fig. 2: The equivalent magnetic circuit of the motor.

3. Structure of the electrical driver

How to realize the electrical driver for parallel-series-windings is also a key point for this switched reluctance based drive. Taking one connection of coil 1 and coil 2 as an example, a simple structure for the electrical driver is given in Fig.3.The half bridge topology that is similar to conventional drivers for SRMs is employed, involving two control switches (S1, S2) that are usually high frequent MOSFETs for low power rate motors and two diodes (D1, D2) for freewheeling of the coils (here are coil 1 and coil 2). Particularly, switch 3 (S3), as shown in Fig.3, is used to realize the parallel-series connection for the motor. For there is no need to act for S3 in a super high frequency, a solid-state relay can be employed to realize the driver. As shown in Fig.3 (b), when S3 turns to the upper points and S1, S2 turn on, the current will pass through coil 1 and coil 2 and the two coils are connected in series. After turning off S2 and S3, diodes D1 and D2 will be activated and then the driver enters a freewheeling mode. Similarly, when S3 turns to the lower points, parallel connection for the two coils can be realized as shown in Fig.3 (c). When S1 and S2 turn on, the two coils will be connected in parallel and currents will pass through the two coils separately. After the two switches turn off, the driver will enter into a freewheeling mode and the two coils share two diodes. More importantly, the current directions from the two coils are different. The positive terminal and the

negative terminal for the coil 2 should be reversed if we manufacture or connect the coils for the motor. Likewise, this parallel-series connection method can be used for windings as well.

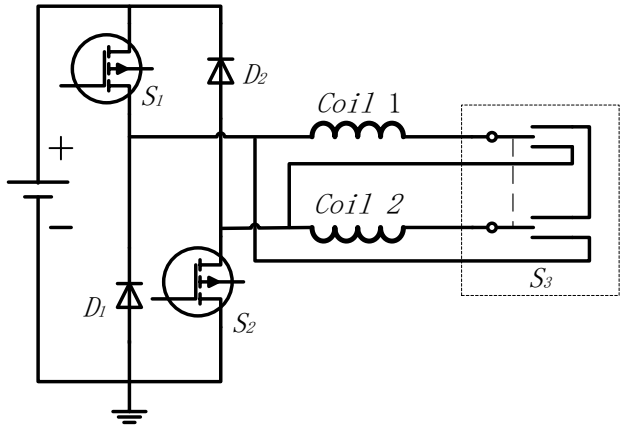

(a)

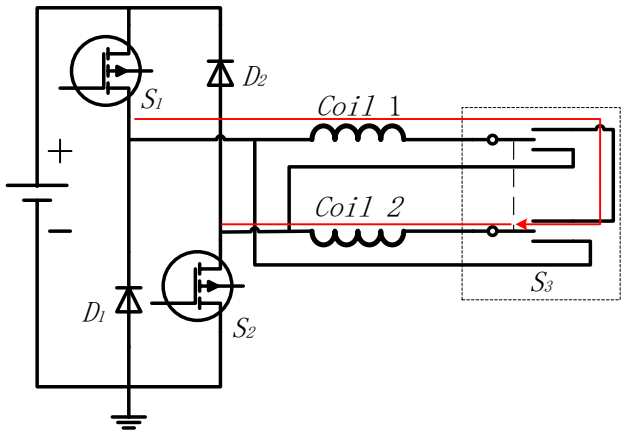

(b)

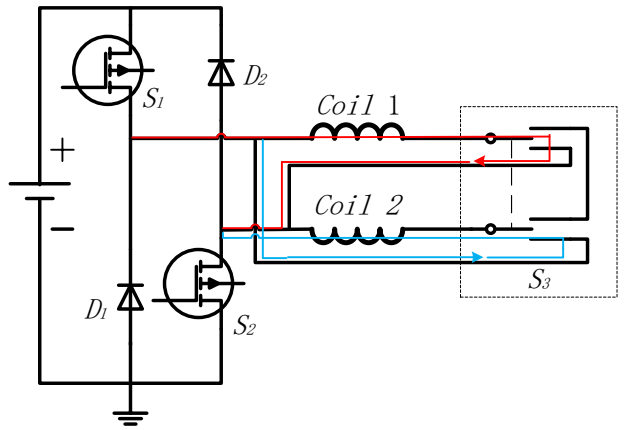

(c)

Fig.3: (a) Structure of the driver to realize the parallel-series connection and (b) the two coils connected in series and (c) in parallel.

4. Mathematical model

The motor obeys the principle of maximum reluctance rule that the poles of the rotor 2 and the teeth of the rotor 1 would coincide with that of the stator. The dynamic equation can be expressed as

$$T_j = J_{mj}\frac{d^2\theta_j}{dt^2} + B_j\frac{d\theta_j}{dt} + T_l = \frac{\partial W_j(i,\theta_j)}{\partial \theta_i} \quad j = 1,2 \tag{3}$$

where, torque T_j is electromagnetic force related to phase currents and angles of the two rotors, J_{mj}, $B_j$and $T_l$are load force, mass of mover and damping coefficient respectively. $W_j(i,\theta_j)$ is co-energy of the motor and θ_j is the angles of the two rotors [10], and j represent the number of rotors.

$$W_j(i,\theta_j) = \int_0^i \lambda(i_j,\theta_j)di_j = \int_0^i L(i_j,\theta_j)i_j di_j \tag{4}$$

$\lambda(i_j,\theta_j)$ is flux linkage of the motor and i_j is the phase current. The value of inductance is a function with phase current and angle of the rotors. According to (3) and (4), we can obtain:

$$T_m = \frac{1}{2}i_j^2\frac{\partial L(i_j,\theta_j)}{\partial \theta_j} \tag{5}$$

It can be seen that the inductance of the rotor is determined by both the current and angle of the rotor and, the torque output is not linearly related with the current as the nonlinear characteristic of the inductance caused by the phase current and angle of the rotor. The electrical terminal for the motor can be expressed as

$$u_j = R_j i_j + \frac{d\lambda(i_j,\theta_j)}{di_j} \tag{6}$$

where, R_j, u_j, and i_j represent phase resistance, terminal voltage and current of phase, respectively.

III. FEM ANALYSIS

1. Electromagnetic field

The magnetic field distributions at aligned angle and unaligned angle for the rotor 1 and the rotor 2 are given in Figure 4. It can be seen from Figure 4 (a) and (b) that the flux is concentrated along the stator and the rotor 1 only. Small poles are designed for the rotor 1 to work at low speeds. When the rotor 1 rotates from un-aligned position to aligned position, flux changes obviously in the yoke of the rotor1 and its teeth. By contrast, the flux distributions of other places roughly keep constant. There is little flux crossing the rotor 2. When the windings are connected in parallel way, long flux path dominant the whole area of the motor as shown in Figure 4 (c) and (d). The flux is distributed along the stator, rotor 1 and rotor 2, and the density of the flux is mainly influenced by the angle of the rotor 2. We can see that the flux in both the stator and the rotor 1 and the rotor 2 changes dramatically at different angles of the rotor 2. With the change of the angles of the rotor1 and rotor 2, the inductance changes will play a main role to generate torque. To realize high speed operation by the rotor 2, its pole width is larger than that of the rotor 1 because of high switching frequent. By doing so, the switching frequent can be reduced due to large electric angle between adjacent phases. Hence, the drive of the motor can be achieved easily.

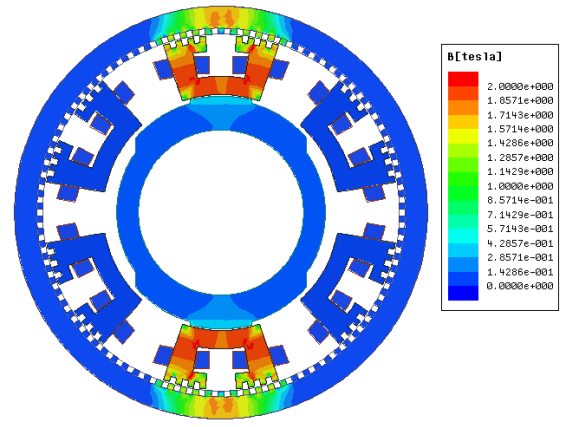

(a)

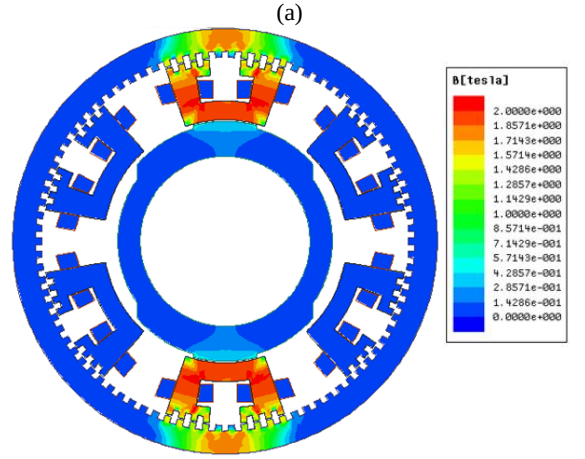

(b)

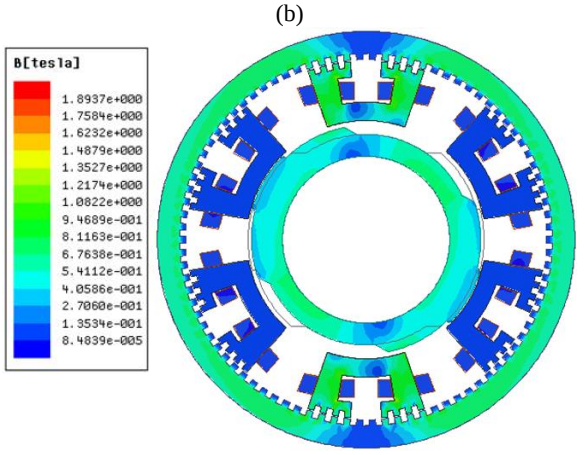

(c)

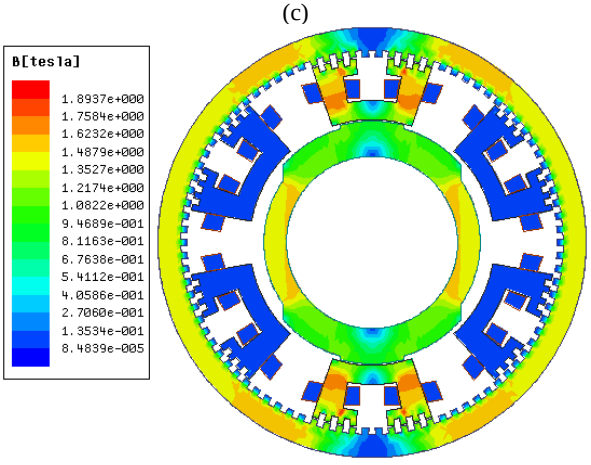

(d)

Fig. 4. Flux density distribution of the motor including (a) short flux path at unaligned angle, (b) short flux path at aligned angle, (c) long flux path at unaligned angle and (d) long flux path at aligned angle.

Inductances and torque outputs with respect to angles are also calculated by FEM as shown in Fig.5. It can be seen from the figure that the values of inductance change dramatically and obviously when the angle of the rotor 1 varies. By contrast, the values experience tiny change when the rotor 2 rotates. Immediately, the latter value is approximately 10 mH less that the former. The average torque output from the rotor 1 is nearly quadrupled than that from the rotor 2. From Fig.5 (d), the torque outputs experience a significant overshoot because of the existence of two lengths of air gaps between the stator and the rotor 2. These torque outputs increase in spite of differing degrees at the beginning with the first air gap increasing from zero to 36 degrees, followed by a sharp drop and then increasing gradually by the degree around 70. Therefore, the second torque outputs are generated from 60 degrees to the end in the whole electrical period of the rotor 2. Rotor 1 can be operated in low speed scope and rotor 2 is suited to realize high speed work.

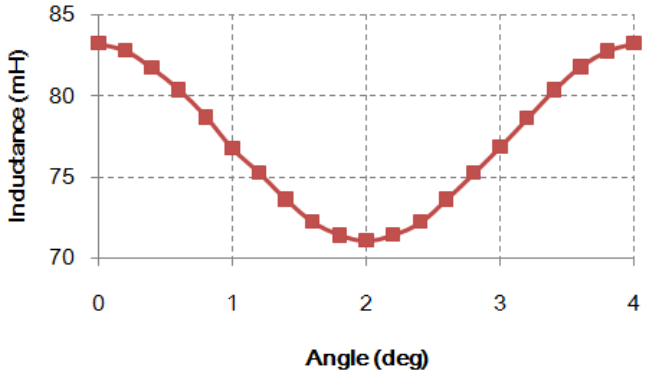

(a)

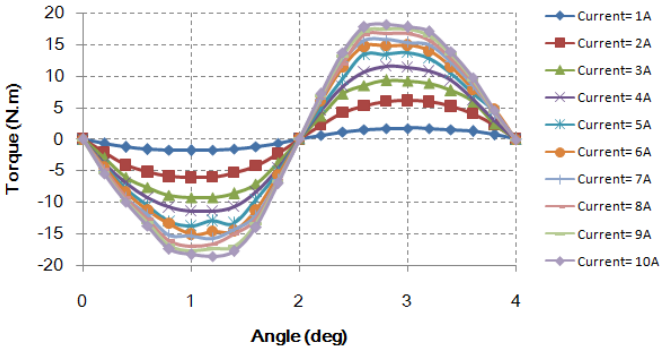

(b)

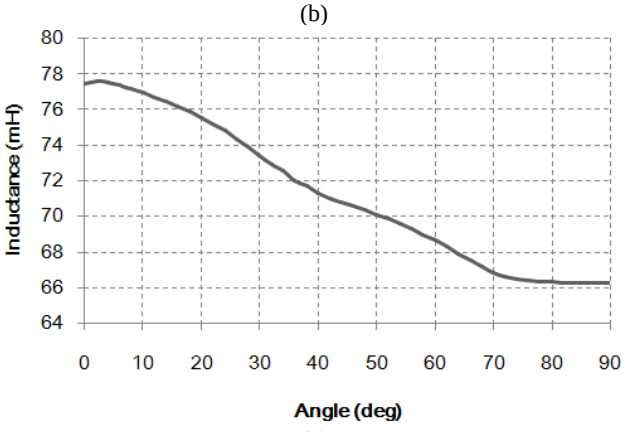

(c)

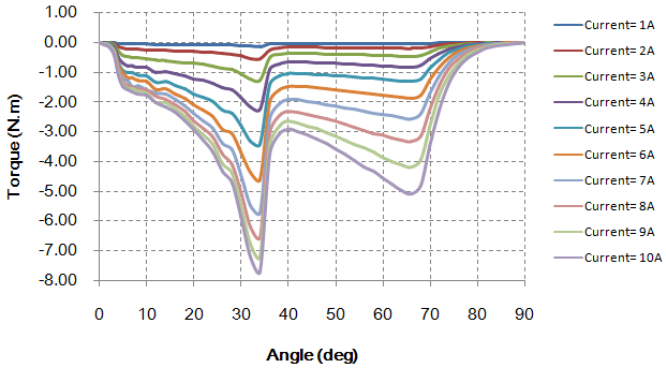

(d)

Fig. 5: Magnetization as a function of applied field.

2. Simulation for parallel-series connection

According to the design of the driver for the motor shown in Fig.3, corresponding simulation modules are built in Fig. 6 (a) to observe the current waveforms when changing the connection status between the two connections. The period of the PWM module is 0.001 s and the period of the pulse is 1 Hz which is used to control the status of the coils connection. It can be seen from Fig. 6 (b), when the series connected coils change to parallel connection, the variations of the two currents of the coils are significant, with the values nearly doubled, experiencing a transient process shown in the circle. The currents can be regulated by the duty of the PWM signal.

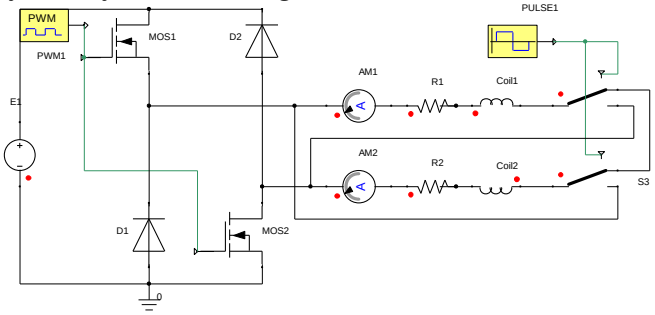

(a)

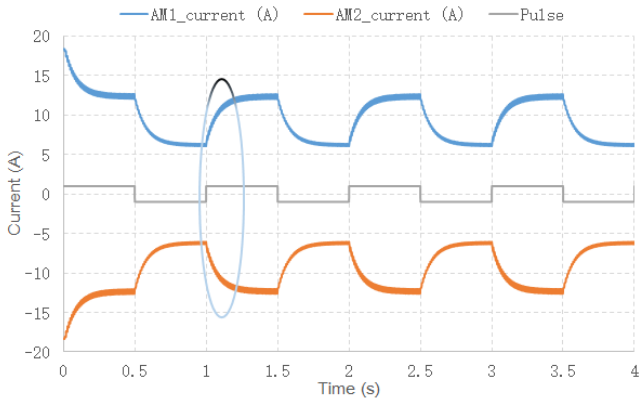

(b)

Fig.6: (a) Parallel-series connection simulation modules and (b) currents of the two coils.

3. Coupling analysis

From the magnetic field distribution of Figure 4, the short path flux fails to pass the rotor 2. Hence, when the rotor 1 works, the flux generated by the windings of the stator could not influence the rotor 2 and they are nearly magnetically decoupled. Figure 7 (a) shows the torque outputs under the same current level 5 A, when the rotor 1 is at unaligned angle and aligned angle respectively. The torque outputs are approximately equal, which suggests that the angles of the rotor 1 has little impact on the torque output contributed by the rotor 2. Similarly, Figure 7 (b) shows the torque outputs of rotor 1 when the rotor 2 is at unaligned and aligned angles, respectively, with the current excitation 2 A. According the calculation results, there is little coupled influence between the rotor 1 and the rotor 2 so that the magnetic coupled effect can be neglected for the control of the motor.

Table 1: Main Specifications of The Motor

Symbol	Conversion from Gaussian and CGS EMU to SI
Rated power	4.2 W
Rated phase current	10 A
Diameter of the rotor 1	140 mm
Diameter of the rotor 2	60 mm
Number of turns of each coil	200
A average Inductance	75 mH
Stack length	100 mm
Speed range	1-10000 rpm

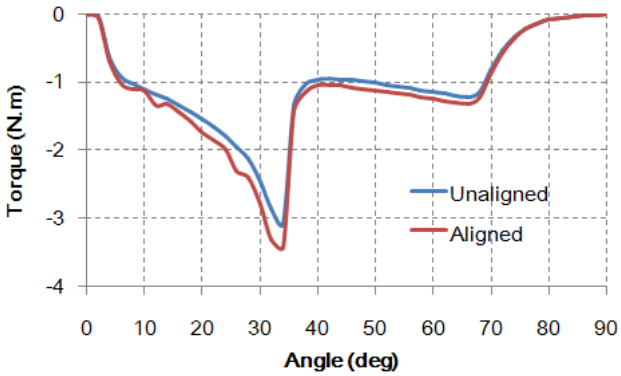

(a)

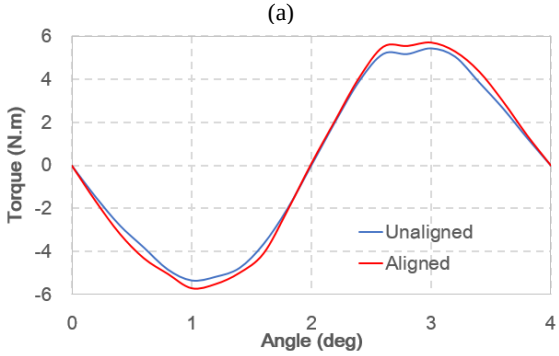

(b)

Fig. 7: (a) Torque output of rotor 2 from aligned angle to unaligned angle when the rotor 1 is at the unaligned and aligned angles and (b)Torque output of rotor 1 form aligned angle to unaligned angle when the rotor 2 is at the unaligned and aligned angles.

IV. Multi-physical Domain Simulation

This section describes the contribution of the paper so that even if readers have not read the body of your paper, they still understand the main idea of the paper. You should not insert any discussion statements in this section because they can be fitted in the previous sections. Even if the author only designed and tested a system, he can also state the achievement in this section. The following statement is

an example: The theory has been implemented in an electronic circuit. The circuit has been prototyped and tested. The experimental results agreed very well with the theoretical prediction and verified the theory proposed.

In order to simulate the real working condition for the motor, the multi-physical domain simulation platform is built and it mainly includes four parts that are electrical part, mechanical part, FEM module and control part, as shown in Fig.8. The electrical part consists of a power supplier, a capacitor and a three-phase asymmetric half bridge topology, comprising the drive for the motor. The mechanical part involves damping and mass elements to set the physical parameters for the motor. The control part is built by using C language module to calculate the current for each phase, according to the feedbacks of angle and angular speed, thus obtaining the turn-on and turn-off angles for the motor in the end. The FEM module is established by using finite element analysis and the basic specifications of the motor are listed in the Table I.

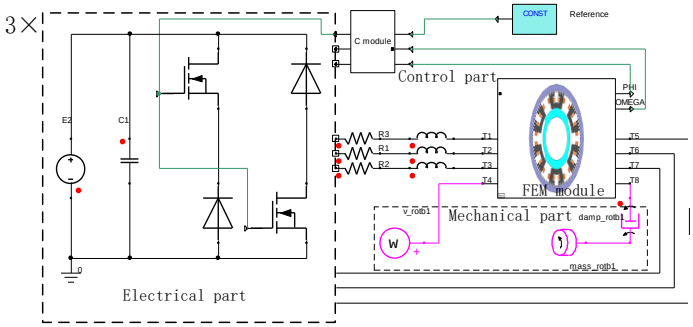

Fig. 8: Multi physical simulation platform for the motor

The speed control block can be simply expressed by Fig.9. It mainly includes three parts that are the controller, the driver and the motor. The controller outputs current reference to the driver after regulating the error of reference angular speed and the real angular speed of the motor. Importantly, for the current regulation part, we select different current regulation methods for high speed and low speed operations of the motor. In high speed, two specific angles are chosen to turn on and turn off the switches during an entire electrical period for each phase. By contrast, the current pulse width modulation (PWM) is employed to regulate the phase currents.

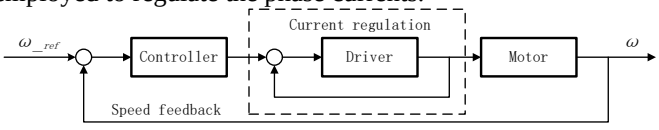

Fig. 9; The speed control block of the motor.

When the motor works in high speed, the torque outputs and speeds are given in Fig.10. From the simulation results, it can be seen that its torque output will decrease with the rise of the speed. From Fig.10 (b), with the speed increases, the load toque experiences high loading torques that exceed 15 Nm, followed by a sharp decline and reach a steady load at average 1 Nm. The speed experiences an acceleration and increases from zero to 10000 rpm, entering a steady status by the end. The results verify that the motor is capable of operation in high speed.

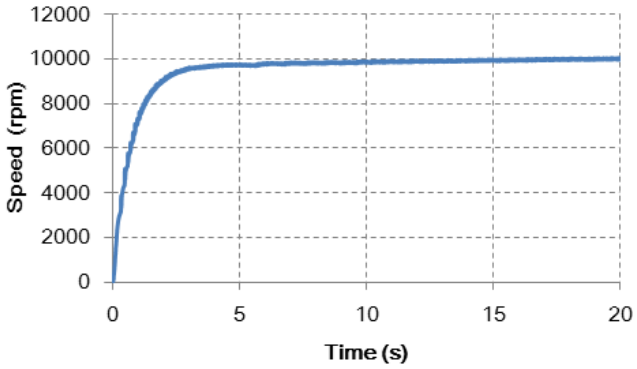

(a)

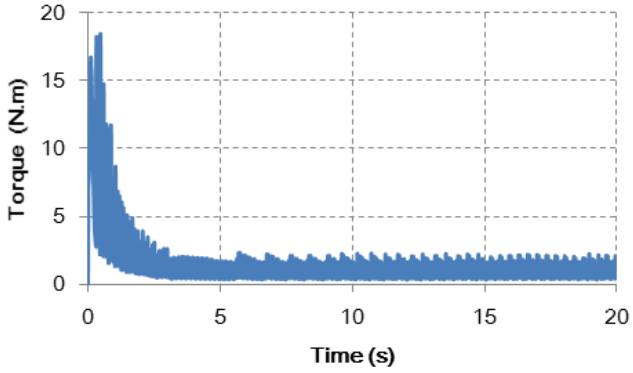

(b)

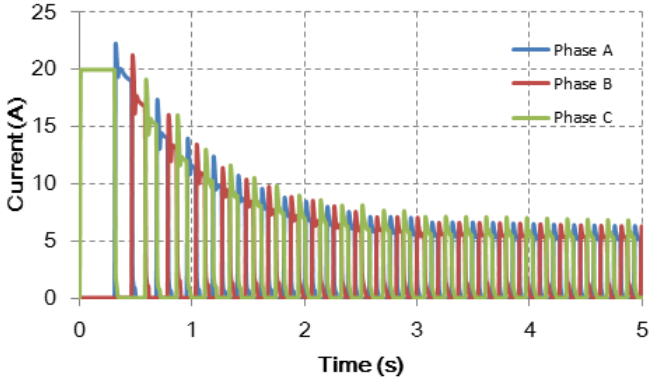

(c)

Fig. 10: (a) the speed curve of the motor with average torque load (b) and currents of three phases (c).

When the motor operates in low speed, the phase currents should be controlled by the method of pulse width modulation (PWM) to curb their maximum values. As shown in Fig.11 (a), the speed waveform and three phase currents indicate the capability of the motor starting with load of 2.5 Nm. By PWM control, currents are regulated at around 6 A, and we can see the accelerating process of the motor, with speed gradually increases from zero to approximate 13.5 rpm within 5 minutes. Fig.11 (b) shows the torque output of the motor under a low speed condition. It can be seen that there is some torque ripple under a low speed working condition for this motor. Although there is some torque ripple in low speed, advanced control algorithms could be developed to mitigate or avoid the ripple. In short, the motor can work in both high speed with angle-position control and low speed with current PWM control.

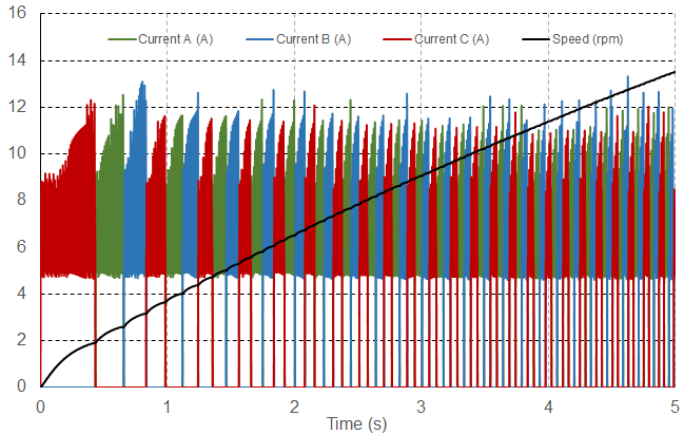

(a)

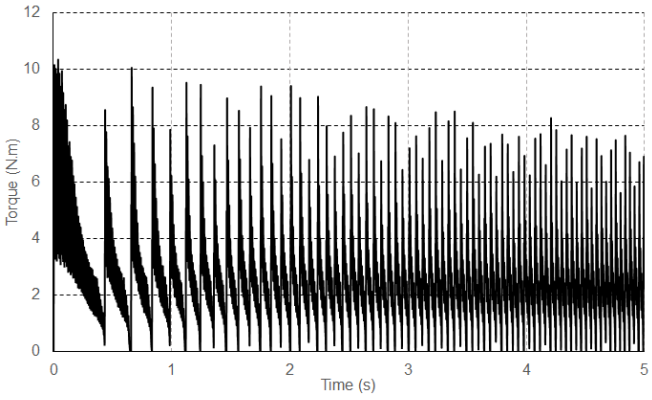

(b)

Fig. 11; (a) the speed and three phase currents with PWM control under load and (b) corresponding torque output.

V. Conclusion

Connecting windings by interchanging parallel and serial circuits is an effective way to integrate double-rotor motors based on switched reluctance principle. Both the theoretical analysis and simulations suggest that by using this approach, the integrated motor with a compact structure is able to realize high and low speeding operations simultaneously, thus achieving a variable transmission for EVs. Meanwhile, finite element analyses confirm that the coupling effect for the motor can be ignored. A forthcoming study on this motor will be carried out, including information on parameter optimizations and manufacturing and controller designs for the motor, etc. The proposed design concept lays a new path for the double-rotor switched reluctance motor that is expected to be employed in EVs, HEVs and Electric Vessels in the future due to its performance in speed and torque.

Acknowledgment

The authors gratefully acknowledge the support from The Research Committee, The Hong Kong Polytechnic University under project reference G-YN27.

References

[1] Joachim Druant, Frederik De Belie, Peter Sergeant and Jan Melkebeek, "Concept Study of a Double Rotor Induction Machine used as Continuously Variable Transmission," IEEE international Electric Machines & Drives Conference (IEMDC), pp.656-661,2015.

[2] Johannes H. J. Potgieter Maarten J. Kamper, "Double PM-Rotor, Toothed, Toroidal-Winding Wind Generator: A Comparison with Conventional Winding Direct-Drive PM Wind Generators Over a Wide Power Range", IEEE Transactions on Industry Applications, vol. 52, no. 4, JULY/AUGUST pp.2881-2890, 2016.

[3] Durmus Uygun, Selim Solmaz, Yucel Cetinceviz, "Dual Stator/Rotor Brushless DC Motors: A Review of Comprehensive Modelling Based on Parametric Approach and Coupled Circuit Model," 2015 Intl Aegean Conference on Electrical Machines & Power Electronics (ACEMP), pp.635-641, sep, 2015.

[4] Zixuan Xiang, Li Quan, Xiaoyong Zhu, and Lin Wang, "A Brushless Double Mechanical Port Permanent Magnet Motor for Plug-In HEVs," IEEE Transactions on Magnetics, vol. 51, no. 11, pp.8111104, 2015.

[5] Yinye Yang, Nigel Schofield, Ali Emadi, "Double-rotor switched reluctance machine design, simulations, and validations," IET Electrical Systems in Transportation, vol.6, no. 2, pp.117-125, 2016.

[6] Zixuan Xiang, Xiaoyong Zhu, Li Quan, Yi Du, Chao Zhang, Deyang Fan, "Multilevel Design Optimization and Operation of a Brushless Double Mechanical Ports Flux-Switching Permanent Magnet Motor", IEEE Transactions on Industrial Electronics, 2016 (early access)

[7] Yinye Yang, Nigel Schofield, and Ali Emadi, "Double-Rotor Switched Reluctance Machine (DRSRM)," IEEE Transactions on Energy Conversion, vol. 30, no. 2, pp.671-680, JUNE 2015.

[8] Chuang Yu, Shuangxia Niu, S. L. Ho, and W. N. Fu, "Magnetic Circuit Analysis for a Magnetless Double-Rotor Flux Switching Motor," IEEE Transactions on Magnetics, col. 51, no. 11, pp.8111905, NOVEMBER 2015.

[9] Anbin Chen; Xiaokun Liu; Fengyu Xu; Jiwei Cao; Liyi Li, "Design of the Cryogenic System for a 400 kW Experimental HTS Synchronous Motor", IEEE Transactions on Applied Superconductivity, 2010, Vol. 20, Issue 3, pp. 2062 – 2065.

[10] T. J. Miller, Electronic control of switched reluctance machines, Newnes Power Engineering Series: U.S., pp.68-72, 2001.

Biography

Li Siyang obtained his BSc degrees from the South China University of Technology in 2012. He is currently pursuing his Ph.D degree under the supervision of Professor Cheng at the Power Electronics Research Centre in the Hong Kong Polytechnic University.
Her research interest mainly focuses on the, Energy conversion, Solar tracking system for CPV power generation system, Design and control the SR motor, as well as energy storage,

K.W.E.Cheng obtained his BSc and PhD degrees both from the University of Bath in 1987 and 1990 respectively. Before he joined the Hong Kong Polytechnic University in 1997, he was with Lucas Aerospace, United Kingdom as a Principal Engineer.
He received the IEE Sebastian Z De Ferranti Premium Award (1995), outstanding consultancy award (2000), Faculty Merit award for best teaching (2003) from the University and Silver award of the 16th National Exhibition of Inventions. He has published over 200 papers and 7 books. He is now the professor and director of Power Electronics Research Centre.

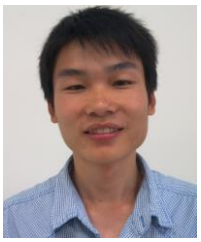

Yu Zou obtained his B.S. degree from Hubei University in 2010 and Master degree at College of Mechatronics and Control Engineering at Shenzhen University in 2013. He is now pursuing his Ph.D degree at The Hong Kong Polytechnic University.